Biosensors and Bioelectronics 37 (2012) 88–93

Contents lists available at SciVerse ScienceDirect

Biosensors and Bioelectronics

journal homepage: www.elsevier.com/locate/bios

Comparison of the direct electrochemistry of glucose oxidase immobilized on the surface of Au, CdS and ZnS nanostructures

Jian Du, Xiuping Yu, Junwei Di*

College of Chemistry, Chemical Engineering and Material Science, Soochow University, Suzhou, Jiangsu 215123, PR China

ARTICLE INFO

Article history:
Received 16 February 2012
Received in revised form
10 April 2012
Accepted 29 April 2012
Available online 8 May 2012

Keywords:
Biosensors
Glucose oxidase
Gold nanoparticles
CdS nanoparticles
ZnS nanoparticles

ABSTRACT

A comparison of the electrochemical and photoelectrochemical behaviors of three biosensors, based on the use of Au, CdS, and ZnS nanoparticles–glucose oxidase (GOD) system, is discussed. All the nanoparticles were electrodeposited onto the indium tin oxide (ITO) thin film coated glass surface. GOD was then immobilized on the nanoparticles-modified electrodes surface with the sol–gel technique. The deposited nanoparticles on ITO electrodes were characterized by scanning electron microscopy, UV–vis spectroscopy and electrochemical impedance spectra. The direct electrochemistry of GOD, analytical performance of glucose calibration curves and the kinetic parameters of the enzyme reaction were compared for all the electrochemical biosensors. Furthermore, the current response of the quantum dots–GOD system biosensor can be increased after illumination. The electrochemical and photoelectrochemical biosensors based on ZnS nanostructures exhibited higher sensitivity than that of Au or CdS nanostructures. Considering ZnS is nontoxic to human and environment, the results suggest that ZnS nanoparticles–GOD system seems to be a promising platform for fabrication of novel electrochemical and photoelectrochemical biosensors.

1. Introduction

Nanomaterials have received great attention due to their attractive properties and applications in many areas, including catalysis, sensing, electronics and photonics. The unique properties of these materials have also been effectively exploited in the immobilization of biomolecules especially enzymes for fabrication of electrochemical biosensors, because nanostructures can play an important role in immobilization of biomolecules due to their high effective surface area, enhancement of mass transport, suitable microenvironment and good conductivity (Pumera et al., 2007; Willner et al., 2007; Ansari and Husain, 2011). The nanomaterials could facilitate the direct electron transfer between enzyme and electrode for fabrication of three-generations of electrochemical biosensors. For example, it is well known that gold nanoparticles exhibit excellent conductivity, high catalytic activity and suitable microenvironment for biomolecules. Gold nanoparticles facilitate more efficient electron transfer between enzyme and electrode surface. This has led to wide employment of gold nanoparticles to develop electrochemical biosensors (Zhang et al., 2005; German et al., 2010; Du et al., 2007; Zhao et al., 2006; Liu and Ju, 2003).

Recently, semiconductor quantum dots (QDs) have also received considerable interests in the fields of photoelectrochemical biosensors (Ren et al., 2009; Zheng et al., 2011; Tang et al., 2008; Sun et al., 2009) as well as electrochemical biosensors (Huang et al., 2005; Dai et al., 2008; Qian et al., 2012; Zhou et al., 2005; Gu et al., 2011; Liu et al., 2007; Wang et al., 2009). Among QDs, CdS was most commonly used (Tang et al., 2008; Sun et al., 2009; Huang et al., 2005; Dai et al., 2008; Qian et al., 2012; Zhou et al., 2005). However, CdS is considered to be carcinogenic to humans, and harmful to the kidneys (impairment) and bone (bone weakness) (Fathy and Ichimura, 2005; Miyawaki and Ichimura, 2007). For "green chemistry", ZnS is very suitable as a good substitute of CdS due to its nontoxicity to the human body and low cost. Furthermore, nano-ZnS can be used as electrocatalyst for the decomposition of ethanol (Bredol and Kaczmarek, 2010). However, the studies of electrochemical biosensors based on ZnS nanostructures were scarce (Zhang et al., 2006).

As it is well known, glucose oxidase (GOD) is a homodimer flavoprotein containing two active sites per molecule and catalyzes the oxidation of glucose to gluconic acid by utilizing oxygen as an electron acceptor with simultaneous production of hydrogen peroxide. A great amount of work has been devoted to construction of various kinds of biosensor based on GOD (Wang, 2008). Thus the GOD was used for the design of electrochemical glucose biosensor model in this work. The goal of this study is to compare the behavior of electrochemical reactivity and analytical performance of three enzyme biosensors composed of different nanoparticles (AuNPs, CdSNPs and ZnSNPs). These nanoparticles were electrodeposited directly onto indium tin oxide (ITO) electrode surface without using any surfactant or organic ligands. Then GOD was immobilized on

* Corresponding author. Tel.: +86 512 65880354; fax: +86 512 65880089.
E-mail address: djw@suda.edu.cn (J. Di).

0956-5663/$ - see front matter © 2012 Elsevier B.V. All rights reserved.
http://dx.doi.org/10.1016/j.bios.2012.04.044

the surface of modified electrodes with the sol–gel technique. The nanoparticles–GOD system is evaluated by comparison of cyclic voltammograms, electron transfer rate constant, Michaelis–Menten constant, and calibration of glucose detection.

2. Experimental

2.1. Reagents

Glucose oxidase (GOD, EC 1.1.3.4, from *Aspergillus niger*, 155 U/mg) was purchased from Sigma. Zinc chloride ($ZnCl_2$) and chloroauric acid trihydrate ($HAuCl_4 \cdot 3H_2O$) were obtained from Sinopharm Chemical Reagent Co., Ltd. Cadmium chloride ($CdCl_2$), sodium thiosulphate ($Na_2S_2O_3$) and glucose were purchased from Shanghai Chemical Reagent Company (Shanghai, China). PVA stock solution of 0.25% was prepared by dissolving polyvinyl alcohol (PVA-124, average degree of polymerization was 2400–2500, Shanghai Chemical Reagent Plant imported from Japan). All other chemicals were of analytical grade and all the solutions were prepared using double-distilled water.

2.2. Deposition of nanoparticles on ITO substrate

All nanoparticles were prepared by the electrochemical method according to previous reports with modifications (Hu et al., 2011; Ghenescu et al., 2008; Loglio et al., 2004). Briefly, a sheet of ITO glass (1.1 mm thickness, less than 100 Ω, Suzhou NSG Electronics Co., Ltd., China) was ultrasonicated with dilute ammonia, absolute ethanol and deionized water for approximately 5 min, subsequently. All the nanoparticles were electrodeposited onto the ITO substrate using cyclic voltammetry at scan potential rate of 50 mV/s. For preparation of AuNPs, the clean ITO sheet was immersed in the solution composed of 0.2 mM $HAuCl_4$ and 0.02 M phosphate buffer solution (pH 7.0). The solution was deoxygenated by bubbling N_2 for 10 min and maintained under nitrogen atmosphere. The deposition was performed in the potential range from 0.1 to −0.9 V for 20 cycles.

The CdS nanoparticles were electrodeposited in the mixed solution containing 0.8 mM $Na_2S_2O_3$ solution and 0.05 M $CdCl_2$ (adding HCl to adjust pH between 2 and 3) at 50 °C. The electrolysis was carried out in the potential range from −0.4 to −0.8 V for 40 cycles. Similarly, the ZnS nanoparticles were prepared in the solution containing 0.08 mM $Na_2S_2O_3$ solution and 0.05 M $ZnCl_2$ (pH about 4) at 50 °C. The condition of electrolysis was in the potential range from −0.4 V to −1.0 V for 40 cycles.

2.3. Preparation of the biosensors

The silica sol was prepared by the ion-exchange method according to the previous literature (Di et al., 2004). After rinsing with water, the nanoparticles modified ITO electrode was dipped in the mixed solution containing 0.3 mL of 1000 U/mL GOD, 0.3 mL of silica sol, and 0.1 mL of 0.2% PVA in each millimeter. Then, the electrode was dried under nitrogen atmosphere for 4–5 h at room temperature. All prepared enzyme electrodes were stored at 4 °C when not in use.

2.4. Instruments and measurements

UV–vis absorption spectra of the nanoparticles were recorded against bare ITO glass as reference using a TU-1810 spectrophotometer (Beijing, China) at room temperature. SEM analysis was carried out with a Hitachi S-4700 scanning electron microscope. Cyclic voltammetry (CV) and electrochemical impedance spectroscopy (EIS) experiments were performed with a CHI 820B (Shanghai Chenhua Apparatus Inc., China) and RST 5200 electrochemical Workstation (Suzhou Risetest Instrument Co., Ltd., China), respectively. The bare ITO and modified ITO electrodes were used as working electrode, a platinum wire as counter electrode and a saturated calomel electrode (SCE) as reference electrode. CV measurements at biosensors were carried out in 0.1 M phosphate buffer solution (pH 7.0). EIS measurements were performed in the presence of 5 mM $Fe(CN)_6^{3-/4-}$ and 0.1 M KCl in the frequency range between 0.1 and 100 kHz at the potential of 0.2 V. The photoelectrochemical measurements were performed under irradiation (350 W xenon lamp).

3. Results and discussion

3.1. Characterization of nanoparticles modified ITO electrode

The performance of the enzyme electrode was greatly affected by the physical morphology of the nanoparticles on substrate surface. The surface morphologies of the Au, CdS, and ZnS nanoparticles modified ITO electrode were characterized by UV–vis spectroscopy and SEM (Fig. 1). The color of Au, CdS, and ZnS nanoparticles deposited on ITO substrate surface was orange, yellow and colorless, respectively. The localized surface plasmon resonance (LSPR) peak of AuNPs was located at about 580 nm with a broad band (Fig. 1A). This is attributed to the assemblage of closely packed AuNPs, which lead to the appearance of the coupled plasmon absorbance of AuNPs (Khatri et al., 2008; Yu et al., 2011). It can be observed from the SEM image (Fig. 1B). The AuNPs were densely distributed on the ITO electrode surface with an average size of about 30 nm. CdS nanoparticles deposited on ITO electrode surface appear more uniform and smooth than those of ZnS (Fig. 1C and D). The rough surface of nanoparticles may be more favorable for immobilization of enzyme.

Electrochemical impedance spectroscopy (EIS) is a powerful technique for studying the interface properties of electrode surface. The EIS spectra, presented as Nyquit plot (Z' versus Z''), at bare ITO, AuNPs/ITO, CdSNPs/ITO, and ZnSNPs/ITO electrodes in 0.1 M $Fe(CN)_6^{3-/4-}$ solution are shown in Fig. 2. Obviously, significant differences in the impedance spectra are observed at different electrodes. The charge transfer resistance (R_{ct}) value between the redox couple and the ITO, AuNPs/ITO, CdSNPs/ITO, and ZnSNPs/ITO electrodes were estimated to be 394, 365, 406 and 413 Ω, respectively. The R_{ct} value on the AuNPs/ITO was remarkably decreased after the nanoparticles were grown onto the ITO. However, the R_{ct} values at the CdSNPs/ITO and ZnSNPs/ITO were slightly increased after the nanoparticles were deposited. This conclusion was supported by the good conductivity of AuNPs and semiconductor of CdSNPs or ZnSNPs.

3.2. Direct electrochemistry of the GOD-based biosensors

Cyclic voltammetry was then employed to characterize the different enzyme electrodes. Fig. 3 displays the performance of the GOD immobilized on bare ITO and Au, CdS, and ZnS nanoparticles modified ITO electrode surface in 0.02 M PBS (pH 7.0) at the scan rate of 100 mV/s. No marked peaks occurred on GOD/ITO electrode. However, all three nanoparticle–GOD electrodes exhibited two well-defined redox peaks with the peak-to-peak separation of about 30 mV. The formal potential (E°) was about −0.45 V, which was consistent with the previous reports (Liu and Ju, 2003; Huang et al., 2005). However, the peak currents at various nanoparticle–GOD electrodes were different. Among the three nanoparticles, the trend of electrode activity was as follows: ZnS > CdS > Au.

At low potential scan rate (< 0.5 V/s), both the cathodic and anodic peak currents were linearly proportional to the scan rate at all enzyme electrodes, which indicated a surface-controlled

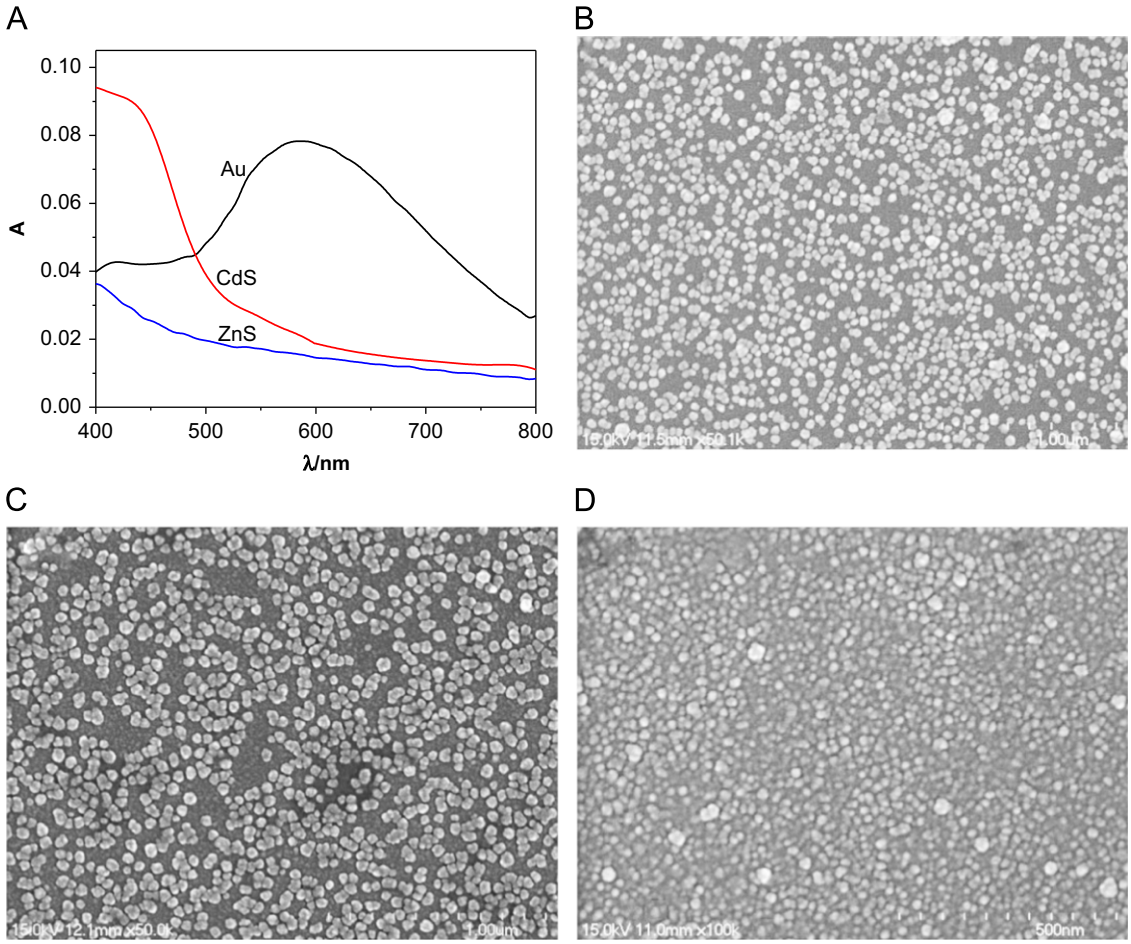

Fig. 1. UV–vis spectra of Au, CdS and ZnS nanoparticles (A) and the typical SEM images of Au (B), CdS (C) and ZnS (D) nanoparticles deposited on ITO substrate.

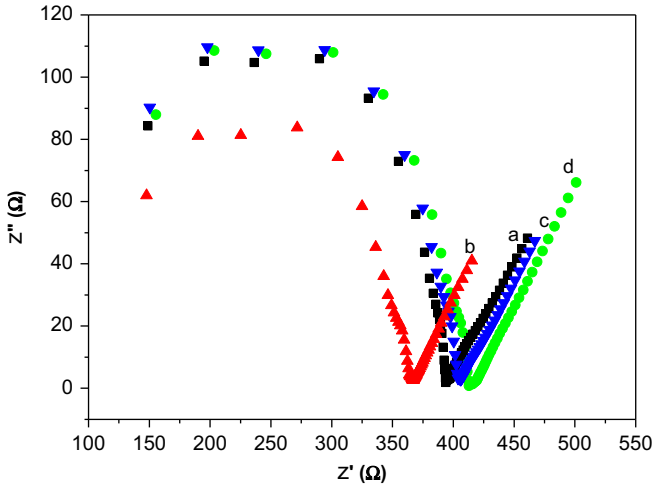

Fig. 2. EIS at bare ITO (a), AuNPs/ITO (b), CdSNPs/ITO (c) and ZnSNPs/ITO (d) electrodes in 5 mM $Fe(CN)_6^{3-}/Fe(CN)_6^{4-}$ (1:1) and 0.1 M KCl solution. Applied potential: 0.2 V; frequency range: 0.1–100 kHz.

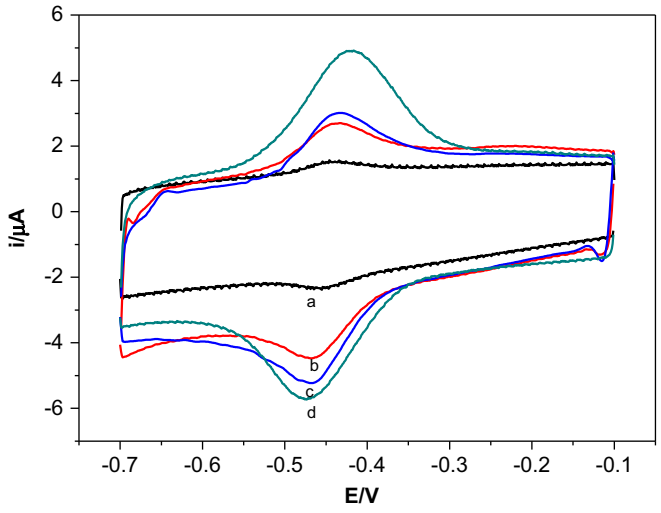

Fig. 3. Cyclic voltammograms at the GOD/ITO (a), GOD/AuNPs/ITO (b), GOD/CdSNPs/ITO (c) and GOD/ZnSNPs/ITO (d) electrodes in 0.02 M PBS (pH 7.0) at the scan rate of 100 mV/s.

electrode surface. At high potential scan rate (> 1 V/s), both cathodic and anodic peak potentials depended linearly with the logarithm of scan rate. An estimation of the electron transfer rate constant (k_s) has been made from the peak potential changes using the Laviron equation (Laviron, 1979). The electron transfer rate constant k_s at Au, CdS, and ZnS nanoparticles modified electrodes was 3.8, 6.1, and 5.7 s^{-1}, respectively. This suggests that ZnSNPs and CdSNPs are more favorable than AuNPs for the facilitation of direct electron transfer between GOD and electrode.

3.3. Optimization of electrodeposition of nanoparticles

As aforementioned in the experimental section, metal and semiconductor nanoparticles were prepared by cyclic voltammetric

deposition because more appropriate size and high particle density of nanoparticles could be obtained. The potential scan rate was fixed generally at 50 mV/s. For cyclic voltammetric deposition, the adjustable parameters were the potential range and cyclic number of potential scan. The cathodic peak current of GOD (Fig. 4) observed at various enzyme electrodes was used as the criterion to assess the performance of the nanoparticles-electrodeposited electrodes that were formed by employing different electrolysis conditions. When the anodic switching potential and scan rate were fixed, the experimental date indicated that the cathodic peak current of GOD at three enzyme electrodes increased first and then decreased with negatively shifting the cathodic switching potential (Fig. 4A). This result was expectable because more nanoparticles should be formed on the ITO electrode surface when a more negative switching potential was employed. However, the nanoparticles were seriously aggregated on the ITO electrode surface with over negatively shifting the cathodic switching potential, which resulted in decreasing the effective surface area of nanoparticles. For example, this phenomenon was clearly observed from the SEM images for CdS electrodeposition at different cathodic switching potential (Supplementary information Fig. S1).

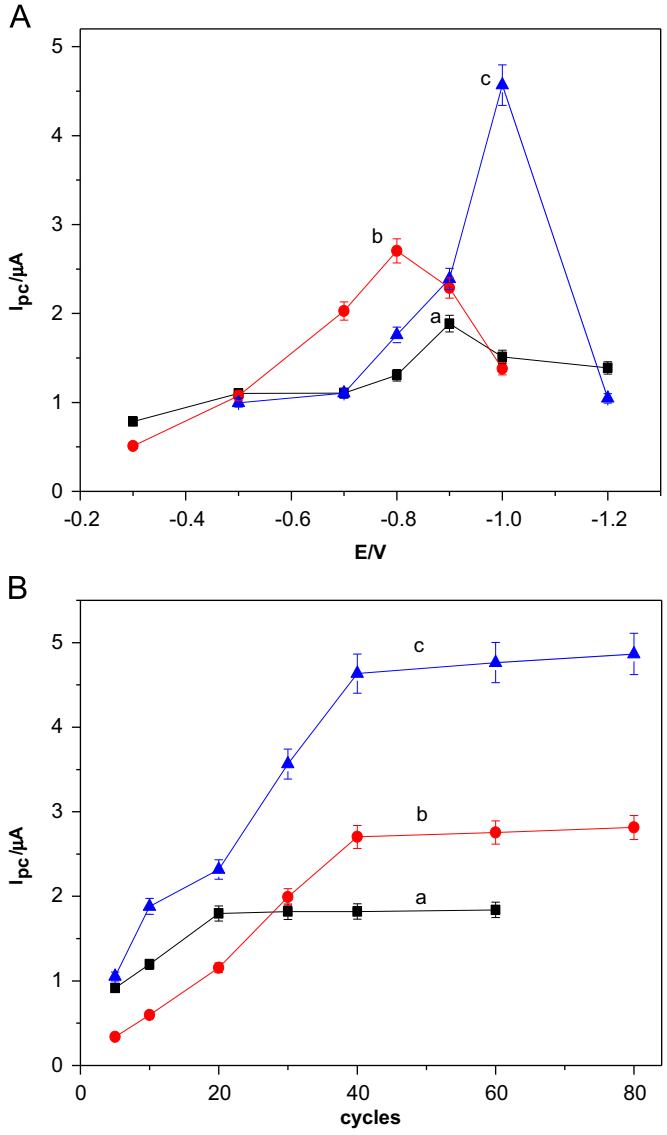

Fig. 4. Dependence of cathodic peak current on the cathodic switching potential (A) and electrodeposition cycles (B) in the electrodeposition preparation of GOD/AuNPs/ITO (a), GOD/CdSNPs/ITO (b), and GOD/ZnSNPs/ITO (c) electrodes.

Fig. 4B shows the effect of the cyclic number of potential scan on the different cathodic peak current of GOD at three enzyme electrodes. The change tendency for the three enzyme electrodes was similar, regardless of the difference of the reduction currents. The cathodic peak current increased first and then reached a plateau. As the cycle number of electrodeposition process increases, the size of formed particles would increase. Accordingly, more surface area will be exposed to the reaction medium to increase Ipc. The increased size with agglomeration of CdS deposits above 40 cycles decreases this area, thus stabilizing the resulting current density. Fig. S2 indicates clearly the changes for the CdS electrodeposition at different cycle numbers.

In order to evaluate the effect of particle morphology on the electrochemical response at QDs–GOD electrodes, another 4-cycle electrodeposition of ZnS and CdS were decorated on the CdSNPs and ZnSNPs surface, respectively. They are defined as CdS–ZnS and ZnS–CdS nanostructures. Then the GOD was immobilized on these QDs modified ITO electrodes by the same procedure. The comparison of the cathodic peak current of GOD was shown in Fig. S3. The maximum cathodic peak current of GOD was obtained from the ZnSNPs–GOD electrode. This further suggests that ZnSNPs are more favorable than CdSNPs for the facilitation of electron transfer between enzyme and electrode.

3.4. Biocatalytic activity of GOD and response to glucose

It is known that the reduction of dissolved oxygen for GOD was a convincing proof of the biocatalytic activity of GOD immobilized on an electrode surface. Fig. 5 displays the cyclic voltammograms of three nanoparticles–GOD electrodes in N_2-saturated (a), oxygen-saturated (b) and oxygen-saturated containing 1 mM glucose (c) in 0.02 M PBS (pH 7.0) at a scan rate of 0.1 V/s. All shapes of cyclic voltammograms for the direct electron transfer of GOD changed dramatically with an increase of reduction peak current and decrease of oxidation peak current (curve a and b in Fig. 5). This is because the reduction form of GOD eletrocatalyzed the reduction of oxygen dissolved in the solution and resulted in a great increase in the cathodic peak current (Liu and Ju, 2003). As well known, in the presence of glucose, the electrocatalytic reaction is restrained due to the enzyme-catalytic reaction and decrease the concentration of the oxidized form of GOD on the electrode. Thus, with the addition of glucose to oxygen-saturated solution, the cathodic peak current of the nanoparticles–GOD electrodes decreased (curve c in Fig. 5). The decrease of the cathodic peak current can be used to determine the glucose concentration. Fig. 5D displays the calibration curves of GOD/AuNPs/ITO, GOD/CdSNPs/ITO and GOD/ZnSNPs/ITO electrodes, with the sensitivity of 0.29, 0.35 and 0.54 uA/mM, respectively. The apparent Michaelis–Menten constant (k_m) at Au, CdS and ZnS nanoparticles platform was calculated to be 7.5, 7.0 and 3.8 mM, respectively. These results suggest that the semiconductor nanostructure, especially ZnS nanoparticles, might enhance the electron transfer reactivity of GOD.

3.5. Photoelectrochemical performance of QDs–GOD based electrodes

The photoelectrochemical properties of the QDs–GOD electrodes were also investigated. The photocurrents were recorded in the 0.02 M PBS (pH 6), while the light of a xenon lamp was used to induce the photocurrent. All QDs–GOD systems generated outstanding photocurrents upon illumination (Inset of Fig. 6). The photocurrent increased immediately upon illumination and retuned back to its original value when the light was turned off.

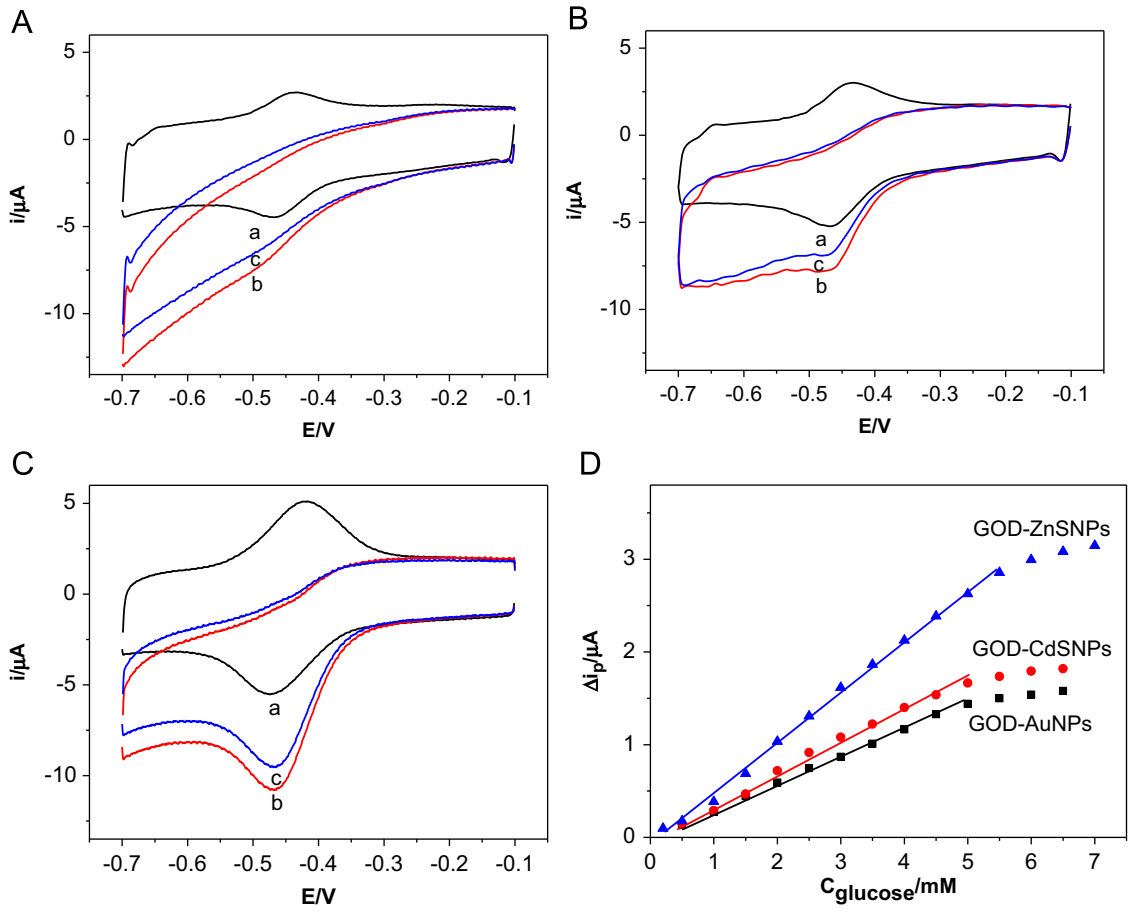

Fig. 5. Cyclic voltammograms of GOD/AuNPs/ITO (A), GOD/CdSNPs/ITO (B), and GOD/ZnSNPs/ITO (C) electrodes in N_2-saturated buffer solution (a), air-saturated buffer solution (b), and air-saturated buffer solution after addition of 2 mM glucose (c) at scan rate of 100 mV/s. Relationship between the decreased current of the reduction peak currents of enzyme modified electrodes and the concentration of glucose (D).

Furthermore, the current response of the ODs–GOD systems to glucose under illumination was also investigated, comparing with the value obtained without illumination. Fig. 6 shows the calibration curves for the measurement of glucose at two different enzyme electrodes under light off and light on, respectively. The sensitivity of the GOD/CdSNPs/ITO and GOD/ZnSNPs/ITO electrodes increased approximate 30% under illumination than without illumination. This indicates that the photovoltaic effect from the CdSNPs and ZnSNPs can improve the catalytic ability of GOD and enhance the response of the enzyme electrode.

3.6. Reproducibility and repeatability of the biosensors

The repeatability of GOD/AuNPs/ITO, GOD/CdSNPs/ITO and GOD/ZnSNPs/ITO electrodes was examined by detecting 0.5 mM glucose for six successive determinations. The relative standard deviation (RSD) is 3.3%, 5.2% and 2.8%, which demonstrate the modified electrodes had good repeatability. The fabrication reproducibility of these three biosensors, made six electrodes independently for each sensor, shows an acceptable reproducibility with the RSD of 4.7%, 5.9% and 4.1%. Then the stability of the sensors was evaluated by monitoring the cyclic voltammetric peak currents of GOD after continuously scanning for 30 cycles. No obvious decrease of the voltammetric response is observed, indicating that the enzyme electrodes were stable in buffer solution.

3.7. Application for the glucose determination

To evaluate the ability of GOD/ZnSNPs/ITO electrode for routine analysis, the determination of glucose in human serum is performed by utilizing the standard addition method. Human serum samples were obtained from the Hospital of Soochow University without any further treatment. The recovery test was performed by adding 0.05 M glucose to the cell in the measurements, which produced the recovery of 96% and 102%, demonstrating good accuracy for the determination of glucose in real samples. The concentration of glucose in two serum samples was obtained to be consistent with those detected by the colorimetric technique in the hospital (Table S1).

4. Conclusions

From the comparison of the behavior of the three nanoparticles–GOD hybrid electrodes, it can be concluded that Au, CdS, and ZnS nanoparticles can promote electron transfer between GOD and electrode. The sensitivity of AuNPs–GOD system is lowest in the three nanoparticles. The electrochemical and photoelectrochemical biosensors based on ZnSNPs are more sensitive and much less toxic to human and environment than that of CdSNPs. Therefore, ZnS nanoparticles seem more favorable than CdS nanoparticles in the fabrication of electrochemical and photoelectrochemical biosensors

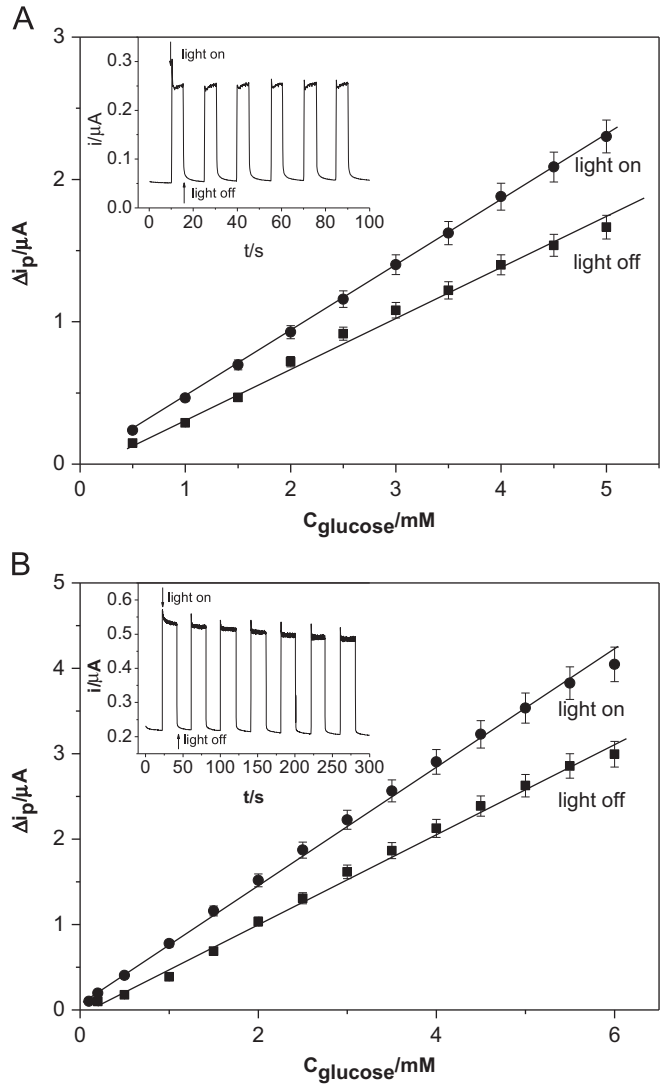

Fig. 6. Calibration curves for the measurements under light off and light on at GOD/CdSNPs/ITO (A) and GOD/ZnSNPs/ITO (B) electrodes. Inset: photocurrent response of the QDs/ITO electrodes in pH 7.0 PBS at applied potential of 0.2 V.

based on QDs–GOD system. This tendency may be extended to the other redox enzyme systems in the application of biosensors.

Acknowledgment

The authors would like to thank the National Natural Science Foundation of China (No. 21075086) and the Priority Academic Program Development of Jiangsu Higher Education Institutions are gratefully acknowledged.

Appendix A. Supporting information

Supplementary data associated with this article can be found in the online version at http://dx.doi.org/10.1016/j.bios.2012.04.044.

References

Ansari, S.A., Husain, Q., 2011. Biotechnology Advances http://dx.doi.org/10.1016/j.biotechadv.2011.09.005.
Bredol, M., Kaczmarek, M., 2010. Journal of Physical Chemistry A 114, 3950–3955.
Dai, Z., Bai, H., Hong, M., Zhu, Y., Bao, J., Shen, J., 2008. Biosensors and Bioelectronics 23, 1869–1873.
Di, J., Bi, S., Zhang, M., 2004. Biosensors and Bioelectronics 19, 1479–1486.
Du, Y., Luo, X., Xu, J., Chen, H., 2007. Bioelectrochemistry 70, 342–347.
Fathy, N., Ichimura, M., 2005. Solar Energy Materials and Solar Cells 87, 747–756.
German, N., Ramanaviciene, A., Voronovic, J., Ramanavicius, A., 2010. Microchimica Acta 168, 221–229.
Ghenescu, M., Ion, L., Enculescu, I., Tazlaoan, C., Antohe, V.A., Sima, M., Enculescu, M., Matei, E., Neumann, R., Ghenescu, O., Covlea, V., Antohe, S., 2008. Physica E 40, 2485–2488.
Gu, Z., Yang, S., Li, Z., Sun, X., Wang, G., Fang, Y., Liu, J., 2011. Electrochimica Acta 56, 9162–9167.
Hu, Y., Song, Y., Wang, Y., Di, J., 2011. Thin Solid Films 519, 6605–6609.
Huang, Y., Zhang, W., Xiao, H., Li, G., 2005. Biosensors and Bioelectronics 21, 817–821.
Khatri, O.P., Murase, K., Sugimura, H., 2008. Langmuir 24, 3787–3793.
Laviron, E., 1979. Journal of Electroanalytical Chemistry 101, 19–28.
Liu, Q., Lu, X., Li, J., Yao, X., Li, J., 2007. Biosensors and Bioelectronics 22, 3203–3209.
Liu, S., Ju, H., 2003. Biosensors and Bioelectronics 19, 177–183.
Loglio, F., Innocenti, M., Pezzatini, G., Foresti, M.L., 2004. Journal of Electroanalytical Chemistry 562, 117–125.
Miyawaki, T., Ichimura, M., 2007. Materials Letters 61, 4683–4686.
Pumera, M., Sánchez, S., Ichinose, I., Tang, J., 2007. Sensors and Actuators B: Chemical 123, 1195–1205.
Qian, J., Yan, S., Xiao, Z., 2012. Journal of Colloid and Interface Science 366, 130–134.
Ren, X., Chen, D., Meng, X., Tang, F., Hou, X., Han, D., Zhang, L., 2009. Journal of Colloid and Interface Science 334, 183–187.
Sun, J., Zhu, Y., Yang, X., Li, C., 2009. Particuology 7, 347–352.
Tang, L., Zhu, Y., Yang, X., Sun, J., Li, C., 2008. Biosensors and Bioelectronics 24, 319–323.
Wang, J., 2008. Chemical Reviews 108, 814–825.
Wang, Z., Xu, Q., Wang, H., Yang, Q., Yu, J., Zhao, Y., 2009. Sensors and Actuators B: Chemical 138, 278–282.
Willner, I., Baron, R., Willner, B., 2007. Biosensors and Bioelectronics 22, 1841–1852.
Yu, X., Wang, L., Di, J., 2011. Journal of Nanoscience and Nanotechnology 11, 11084–11088.
Zhang, F., Li, C., Li, X., Wang, X., Wan, Q., Xian, Y., Jin, L., Yamamoto, K., 2006. Talanta 68, 1353–1358.
Zhang, S., Wang, N., Niu, Y., Sun, C., 2005. Sensors and Actuators B: Chemical 109, 367–374.
Zhao, S., Zhang, K., Bai, Y., Yang, W., Sun, C., 2006. Bioelectrochemistry 69, 158–163.
Zheng, M., Cui, Y., Li, X., Liu, S., Tang, Z., 2011. Journal of Electroanalytical Chemistry 656, 167–173.
Zhou, H., Gan, X., Liu, T., Yang, Q., Li, G., 2005. Journal of Biochemical and Biophysical Methods 64, 38–45.